A smartphone-based laser distance sensor for outdoor environments

Jason H. Gao and Li-Shiuan Peh

***Abstract*— Laser distance sensors such as LIDAR are useful for many outdoor robotic vehicles, but their high cost and complexity precludes their use in low-cost applications, while other low-cost depth sensing technologies are not suitable for outdoor use. We present a low-cost, smartphone-based planar laser distance sensor design for outdoor use with 6 cm accuracy at 5 meters, 30 Hz scan rate, and 0.1 degree resolution over the field of view. The cost of the hardware additions to the off-the-shelf smartphone used in our prototype is under $50.**

I. Introduction

Mobile robots must avoid obstacles when navigating an environment. This is typically done with a laser distance sensor (LDS), which is also often used for localization and mapping [1]. Work on passive camera-based systems can eliminate the need for expensive LDS devices, such as LIDAR, for localization [19], but an LDS is still useful for reliable obstacle detection and avoidance. The high cost and complexity of LDS devices, however, has precluded their use for low-cost applications and handheld use.

We present Smartphone LDS, a low-cost multi-point laser distance sensor, based on a smartphone, that works outdoors. It is designed to leverage off-the-shelf components and the rapid improvement and proliferation of phones with low-cost, high performance image capture and processing. Our prototype, shown in Figure 1, combines a phone with an off-the-shelf line laser module, and leverages the phone's camera, processor, and input/output to simultaneously measure multiple distances across a planar field-of-view. By utilizing the processing power of the phone, we can perform more intensive image processing to identify the laser illumination and reject ambient light, improving performance for outdoor use. Our sensor has the characteristics shown in Table I. To our knowledge, there is no other outdoor 2D laser distance sensor that combines a low-cost laser illumination source with computer vision-based image processing techniques.

Smartphones are increasingly pervasive, and are continuously and rapidly increasing in computing power and sensing capability. This has not gone unnoticed in the robotics community: even Robot Operating System (ROS) is available on Android [11], developed by Google and Willow Garage.

Compared to the typical laser distance sensors utilized in autonomous outdoor robots, smartphones are also low cost: the Android phone used in our system, a Nexus 5, has an original retail price of $349, and the hardware additions for our prototype cost less than $50, as shown in Table II. We believe the additional hardware costs can be significantly reduced in mass production. Thus, adding high-resolution distance sensing to the phone enables a complete robotics platform, including the laser distance sensing and ROS software environment that many researchers are accustomed to, at low cost and in a mobile form factor.

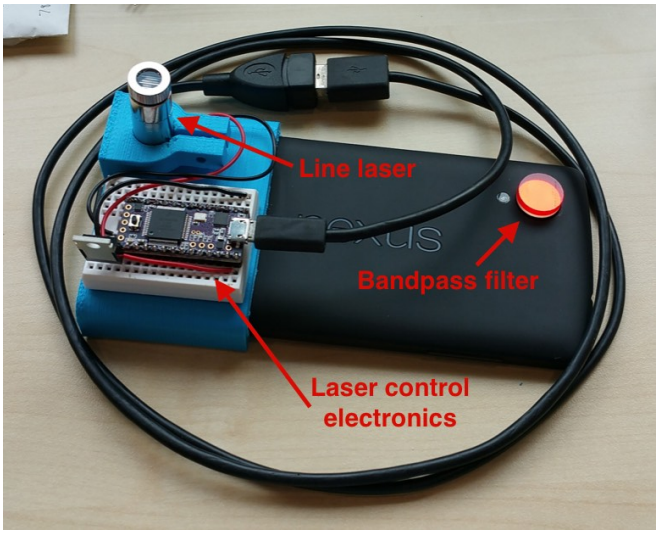

Fig. 1: Smartphone LDS with major components labeled.

TABLE I: Smartphone LDS Characteristics

Works in sunny outdoor conditions under strong ambient light
Solid-state design with no moving parts
Field-of-view of 48 degrees (dependent on camera and laser lens)
Returns range readings up to 2m in direct sunlight, 5.8m indoors
Fast: 14400 readings / second (480 simultaneous readings at 30 Hz)
High minimum angular resolution of 0.1057 degrees
6 cm range error at 5 m
Low cost: Leverages pervasive smartphones & inexpensive off-the-shelf components
Eye-safe

A phone-based LDS enables many applications that were not previously possible, due to its pervasive deployment and low cost. In Section IV, we evaluate our system in the scenario of obstacle detection and avoidance in autonomous vehicles. Other potential applications include obstacle avoidance on lightweight personal mobility vehicles, 3D scanning with phones, navigational aids for the visually impaired through smartphone apps and small autonomous robots utilizing advanced localization and mapping algorithms designed for laser distance sensors.

There are several distinguishing characteristics of our

The authors are with the Computer Science and Artificial Intelligence Laboratory, EECS Department, Massachusetts Institute of Technology, Cambridge, MA 02139, USA (email: jasongao, peh@csail.mit.edu).

*This work was supported by the Singapore National Research Foundation programs SMART Future Urban Mobility and SMART Low Energy Electronic Systems.

Preprint submitted to 2016 IEEE International Conference on Robotics and Automation. Received September 15, 2015.

TABLE II: Smartphone LDS Cost Breakdown

Nexus 5 smartphone	$349
Optical bandpass filter	$13
Line laser	$22
Control electronics	$12
3D-printed mount	$2
Total of hardware additions	**$49**
Total including smartphone	**$398**

design from prior work on low-cost laser distance sensors such as the Revo LDS [12] by Konolige *et al.* In particular, our design:

- **Works outdoors**, as shown in our evaluation in direct sunlight in Section IV-A. We tested the Revo LDS design outdoors by extracting the unit from a Neato XV-11 robotic vacuum cleaner, and were unable to obtain range measurements beyond half a meter when the target surface was illuminated by direct sunlight. The Revo LDS utilizes bandpass filtering and temporal synchronization of the laser illumination with a global shutter CMOS image sensor to reject ambient light, but sunlight is still too strong for it to reliably discriminate the laser light. Our design modulates the laser illumination and leverages relatively powerful heterogenous processing cores on smartphones to perform image-processing across multiple camera frames, improving ambient light rejection.
- **Has a solid-state design** with no moving parts. This makes it lower-cost and more suitable for handheld and/or consumer applications, with simple assembly, no gyroscopic effect from spinning parts, and no moving parts to break or wear out. This is unlike other laser distance sensors that typically use a spinning mirror or electronics to scan the laser and take measurements.
- **Exploits silicon advances readily.** Smartphones are pervasive, and have been rapidly increasing in computing power and camera performance. This means the performance of the system design will improve, and only relatively simple hardware modifications / attachments to the phone are required. For example, better cameras and processors in newer phones will improve the throughput, range resolution, angular resolution, and detection latency and/or lower cost.

II. Background and related works

Addressing the general problem of distance sensing is important for mobile robots that must navigate unstructured environments. We discuss several typical approaches below:

- Laser distance sensors such as LIDAR have the advantage of high spatial resolution, allowing robots to discriminate between multiple types and sizes of obstacles, but its cost is prohibitive for lower-cost systems due to the need for high-speed circuitry for accurate time-of-flight ranging, high-powered laser diodes and photodetectors, and electromechanical components to scan the optics over the field of view.
- Stereo-vision has the advantage of not requiring active illumination, but relies on complicated and intensive computation, and performs poorly in environments that have surfaces lacking textures for the stereo correspondence algorithm to exploit.
- Ultrasound is low cost and commonly used on small mobile robots, but suffers from low range and low spatial resolution [2] that is inadequate for object discrimination and classification.
- Radar has the advantage of measuring an object's relative speed to the sensor in real-time by leveraging the doppler shift effect, but also suffers from poor spatial resolution across the field of view and high cost.

Our design's key contribution is that it is low-cost and works outdoors in sunlight. We use an active triangulation approach. Below, we discuss several related approaches in other active illumination distance sensors.

- **Pulsed Time-of-Flight (ToF).** Systems operating under this principle constitute what is typically considered LIDAR, and include devices such as the SICK LMS 291 and Velodyne 3D LIDAR sensors [6] that are often used in autonomous vehicles research. ToF sensors emit a very short, high-power laser pulse, and measure the time it takes to detect its reflection from a distant surface. The high-power lasers, sensitive photodetectors, high-speed electronics, and scanning optics found in these systems result in prohibitively high cost. Kimoto et. al. [10] developed a 3D LIDAR that is relatively low-cost compared to 3D LIDARs by adding a resonant mirror to a 2D LIDAR, but it still requires moving components and is high cost compared to our approach.
- **Modulated light Time-of-Flight.** SoftKinetic [3] and Kinect for Xbox One [16] both emit high-frequency (10s of MHz) modulated light and measure the phase shift of the return signal due to the time of flight to provide a 3D depth image. However, their ambient light rejection is not strong enough for outdoors use due to the wide divergence of illumination energy both horizontally and vertically. These approaches also require specialized CMOS imagers and control circuitry in order to capture and process signals at high speed.
- **Structured light.** Several commercially available depth sensors utilize structured light, measuring distortions in a projected pattern to determine depth, including Google Project Tango [8] and the original Kinect [9]. Similarly to the modulated light sensors above, they do not perform well outdoors due to ambient light quickly overpowering the sensor's illumination as the energy diffuses in both directions.
- **Active triangulation.** Our design falls under this category of sensors, which use an illumination source and an arrayed image sensor to locate reflected illumination on the image sensor and calculating the distance. Such systems have similar challenges detecting the active illumination in ambient light, which we address in our design.

Preprint submitted to 2016 IEEE International Conference on Robotics and Automation. Received September 15, 2015.

Our system is novel in its use of line laser modulation, image processing, and the full use of a 2D image sensor to enable compact 2D outdoor laser distance sensing with no moving parts. The line laser illumination diverges in only one axis, maintaining laser illumination flux at longer distances, and we improve ambient light rejection through modulation.

The Revo LDS [12] is similarly low-cost and also uses active triangulation, but requires a physically spinning component to scan its single-point sensor over the field of view and does not perform well outdoors (Section IV-A). Our design samples multiple points simultaneously without moving parts. Quigley et. al. [17] also use a line laser for active triangulation, but the system is not suitable for outdoor use and processing of the scans is not done in real-time.

III. Rangefinder Design

Our system is an outdoor, active-triangulation laser distance sensor. It consists of an illuminator and a detector separated by a baseline distance. The illuminator is a laser module with a line lens, and projects a horizontal beam of laser light into the scene. The detector is the camera on the off-the-shelf Android smartphone, capturing images to be processed by the phone's processors (CPU and GPU).

The vertical baseline distance between the camera and the line laser emitter causes laser illumination reflected off objects in the scene to be detected at different vertical positions across the image plane of the camera, depending on the distance to the illuminated object. Thus, each column of pixels in the image corresponds to one measurement within the field-of-view, and we can simultaneously take as many measurements as there are columns of pixels (480 in our prototype, as discussed in Section III-B).

These major components of our system are shown in Figure 1, while a detailed diagram of the hardware and software components of our system is shown in Figure 4.

A. Challenges

There are several competing demands on this system:

- **Eye safety.** The laser needs to be eye-safe due to its outdoor operation, which limits its output power and the maximum range of detection.
- **Processing performance.** The sensor needs to perform image processing from the camera to distinguish the signal of interest (the line laser return) from the background (other objects in the scene, background radiation from the sun, etc.). This processing needs to be done in real-time on a low-cost device.
- **Sensing fidelity.** We have limitations on camera frame rate, dynamic range, and electronic rolling shutter (due to the CMOS image sensor in the phone).

We discuss the impact of possible improvements to our system in Section V.

B. Design Criteria and Characteristics

Because our design leverages several off-the-shelf components, our design must consider the properties of the system that we cannot change:

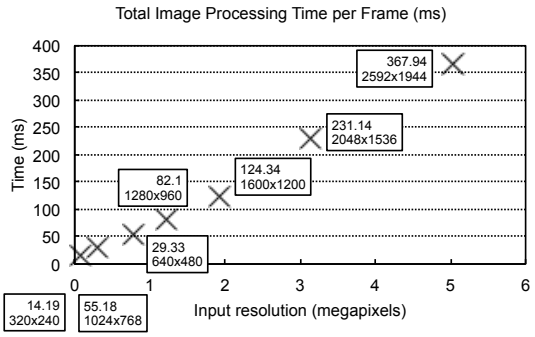

Fig. 2: Total processing time per frame by our app versus image resolution.

- **Phone processor performance.** Figure 2 shows the per-frame total processing time of our image processing kernels versus image resolution. Running at the full frame rate of the camera (30 fps) gives us 33.33 ms to process each frame, so we capture images at 640x480 pixels resolution, down-sampled from the full resolution of the camera, to stay within the limits of the phone's compute performance.
- **Camera frame rate.** The maximum frame rate of the camera is 30 frames per second.
- **Camera sensor physical characteristics.** The camera on the Nexus 5 phone has a focal length of 3.97 mm and physical sensor dimensions of 4.6032 by 3.5168 mm, as reported by the Android Camera2 API. As we are using the longer dimension of the sensor to localize the laser illumination along, each pixel in the down-sampled image corresponds to a physical distance on the sensor of 0.0072 mm.
- **Available baseline separation.** The size of the phone provides a lower bound on the size of the overall system, but an overly large baseline will result in a large system.

The triangulation geometry described in Konolige *et al.* for the Revo LDS also applies to our system, with perpendicular distance to an object from the baseline separation as

$$q = \frac{fs}{x} \tag{1}$$

with x the position of the reflected laser illumination on the CMOS imager. To enable comparison of our Smartphone LDS to Revo LDS, we wish to achieve an fs product comparable to the $fs = 800$ of [12], and thus must maximize our baseline separation, as our focal length is fixed and smaller than that of the Revo LDS. We choose our baseline separation to be 155mm, slightly longer than the length of the phone, in order to keep the system compact, with the laser attached rigidly to the phone via a 3D-printed mount. The resultant $fs \approx 615$ provides us with comparable range resolution and minimum distance as the Revo LDS, while keeping the size of the system small.

To provide readings across the field of view, we use the narrower vertical dimension of the image sensor to triangulate the laser light at multiple angles simultaneously.

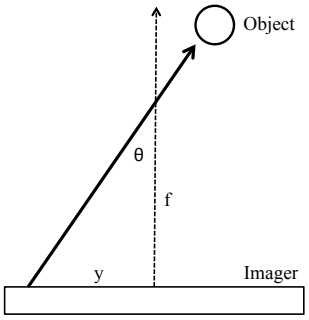

Fig. 3: Geometry of angle to object. The angle θ is calculated from the y position of the laser illumination in the image.

Equation 2 gives the position y of the laser illumination on the image sensor, and

$$\tan\theta = \frac{y}{f} \tag{2}$$

Thus, our angular sensitivity is dependent on the position y on the image sensor and the physical camera characteristics:

$$\frac{d\theta}{dy} = \frac{f}{f^2 + y^2} \tag{3}$$

where dy is the width of a pixel: 3.5168 mm / 480 pixels. Angular resolution is lowest in the center of the field of view, with an angular resolution of 0.1057 degrees, and highest at the edge, with an angular resolution of 0.09513 degrees.

C. Ambient Light Rejection

Typically, the use of a line laser will result in the laser energy being spread out over the line, making it difficult to detect the reflected illumination at longer distances. We add a 20nm bandpass filter to reduce most of the ambient light flux. We also modulate the laser and perform additional processing on the phone to further reject ambient light.

The modulation of the laser is controlled by the smartphone through a microcontroller connected via the Android USB Host API. The laser is pulsed on alternate frames. Due to the electronic rolling shutter on the camera, the laser pulse must last for the entire frame capture duration of 1/30 s, rather than just the image exposure time.

The app tracks per-pixel luminosity transitions between frames and counts how many occur on-off or off-on as expected from knowledge of the laser pulse modulation. When the number of matched transitions detected reaches a threshold (4 in our experiments), the pixel is tagged as having the modulated laser illumination present. Requiring a number of matched transitions imposes a latency penalty of $threshold/framerate$ seconds before a new range reading can be detected. A threshold of 4 imposes a latency of 0.133 seconds, comparable to that of the Revo LDS, which cannot detect an object's distance until it has physically scanned across it. At a 5 Hz scan rate, the latency of the Revo LDS can range from 0 to 0.2 seconds.

This algorithm provides good rejection of ambient noise as shown in Figure 5. The phone is able to process images at 30 Hz, the maximum framerate of the camera. The image processing is accelerated on the CPU and GPU through the use of RenderScript, Android's parallel computing framework.

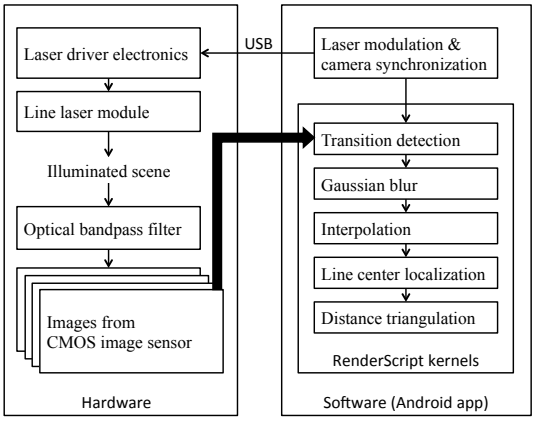

Fig. 4: Block diagram of hardware and software components.

D. Eye-Safety

To prevent distraction to passers-by during our outdoors and vehicle experiments, we chose to use a non-visible wavelength of 780 nm for the illumination. and removed the infrared cut-off filter from the smartphone camera. We add a 20 nm optical bandpass filter to further reduce ambient light, as discussed above. The 100 mW line laser is effectively pulsed at 15 Hz with a 50% duty cycle. The lowest Maximum Permissible Exposure (MPE) is $5.8 \times 10^{-5} J/cm^2$ given by the equation for a repetitively pulsed laser [4]:

$$\frac{1.8 C_a t^{0.75} \times 10^{-3}}{n^{1/4}} \tag{4}$$

where $C_a = 10^{2(0.78-0.7)}$, $t = 1/30s$, and $n = 150$ pulses in 10 s (natural motion of the eye). The power absorbed by the retina if looking directly into the laser beam falls off quickly with distance due to the very wide 60 degree

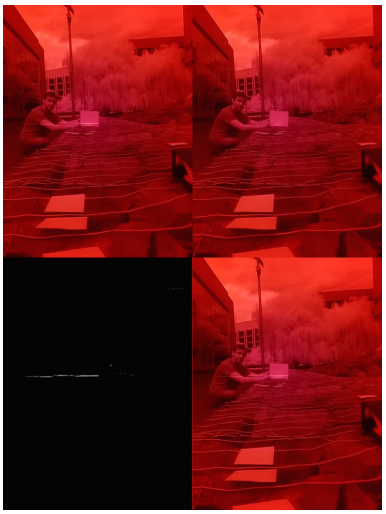

Fig. 5: App screenshot. Detected light in lower left quadrant.

Preprint submitted to 2016 IEEE International Conference on Robotics and Automation. Received September 15, 2015.

horizontal divergence. For safety, we assume all of the energy within the vertical divergence of the beam falls on the retina of the eye and we do not include energy loss through the air. Thus, the minimum eye safe distance or Nominal Ocular Hazard Distance (NOHD) at which the MPE is not exceeded is 1.45 m, given by:

$$A \times MPE = Pt\frac{w}{2D\tan(divergence/2)} \quad (5)$$

where $A = 0.385cm^2$ is the area of the pupil, P is the pulse power, D is the NOHD, and $w = 0.7cm$ is the pupil width (with all of the beam's vertical width falling on the pupil).

There are multiple ways to accomplish this: the system can include an interlock mechanism that reduces the power or disables the laser when a closer object is detected, or for integration into larger systems such as vehicles, a physical shroud around the system can prevent exposure closer than the NOHD. Alternatively, if using a global shutter camera sensor instead, the pulse duration could be reduced from 33.33 ms to the camera exposure time of 3 ms, increasing the MPE 5.6-fold and reducing NOHD to 0.26 m.

E. Laser Line Localization

To localize the laser line within the image, we first gaussian blur the image to spread out saturated pixels to better locate the center of the line in each column of pixels, and then interpolate the image of the line 2x to improve subpixel accuracy along each column. The interpolation is limited by the processing time of our unoptimized prototype software, and affects our range resolution at longer distances. Figure 6 shows total image processing time for other interpolation factors at an input resolution of 640x480. After interpolation, we find the center of the laser light in the row using the maximum value. Finally, to improve the subpixel localization accuracy, we calculate the centroid with the 8 neighboring pixels on each side of the center.

F. Calibration

The range errors of the system primarily come from:

- **The angle between the laser and the camera.** This comes from inaccuracy in the 3d-printed mount, inaccuracy of the low-cost line laser diode alignment, and misalignment and distortion from the line lens on the laser. Due to the use of a line laser with a slightly greater horizontal divergence than the field-of-view of our camera, the system can tolerate misalignment (up to +/- 6 degrees) of the laser within the plane of the emitted line, as a rotation of the laser within that plane still results in pixels across the field-of-view being illuminated with reflected laser light. We manually align the angle of the emitted line itself by rotating the laser module around its longitudinal axis.
- **Residual lens distortion.** The effect of known lens distortion is corrected for by Android's camera software subsystem, but there may be residual distortion due to manufacturing and alignment variation in the camera module.

Similarly to [12], we address these errors by calibrating a 1/x curve fit (Figure 7) between our localized laser positions in the raw image and the distance to a white (greater than 90% reflectivity) calibration target, with more weight given to longer distances because the higher slope results in greatly magnified localization errors. We use an LDS from a Neato XV-11, which is based on the device from [12], to provide our baseline of known distances. The curve fit is imperfect, and errors remain after calibration, shown in Figure 8. To correct for remaining error, we use table of offsets from the actual distance, applied with interpolation above distances of 1.0 m, which eliminates the effects of calibration errors, but subsequent mechanical flex of the 3d-printed mount that enforces the angle between the laser and the camera could cause further calibration errors to manifest.

IV. Performance Evaluation

We evaluated our phone-based laser distance sensor by first characterizing its distance sensing performance outdoors, and then characterizing the system in an example application scenario: obstacle detection for an outdoor autonomous vehicle.

A. Outdoor Distance Sensing Evaluation

We tested Smartphone LDS outdoors by mounting it next to the XV-11 device, depicted in Figure 9, and measured

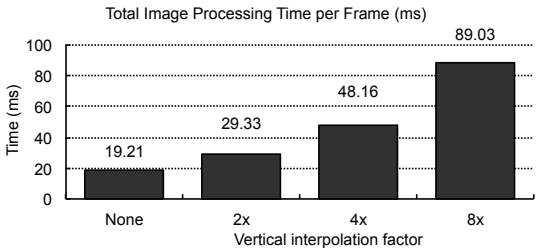

Fig. 6: Total processing time per frame vs. interpolation.

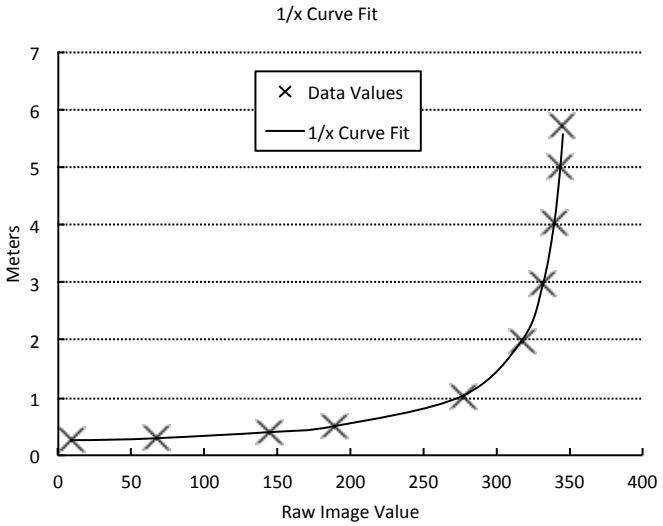

Fig. 7: Calibration readings and 1/x curve fit.

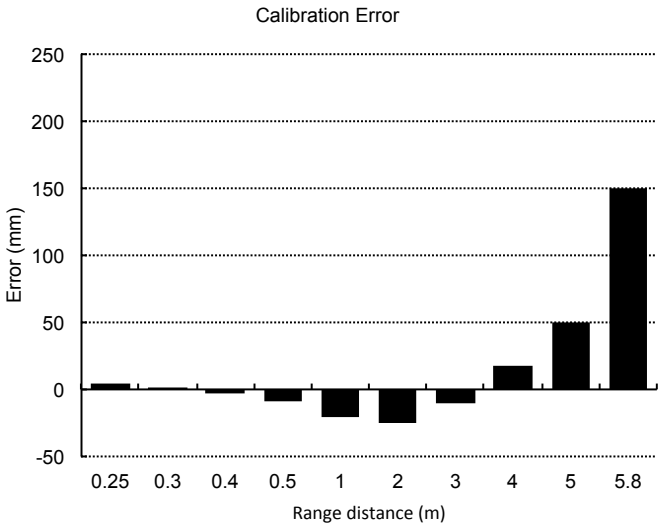

Fig. 8: Calibration error after 1/x curve fit.

range error vs. distance for white targets (90% reflectance) and black targets (10% reflectance) under the following scenarios:

- Outdoors, with target surface shaded from sunlight.
- Outdoors, with target surface under direct sunlight.

Figure 10 shows the maximum range achieved by each system outdoors in our measurements. Smartphone LDS is consistently able to detect further targets than the XV-11.

Figure 11a shows the total error for white and grey targets. We also include the measurements from the calibration for comparison, performed indoors with a white target. Figure 11b shows the XV-11 unit tested under the same conditions for comparison, but we do not have the calibration data for it. Measured errors are comparable to those in [12].

Our standard deviation error remains under 10 mm indoors for all ranges, and under 2 mm outdoors to 1 meter. At 3 meters, Smartphone LDS was unable to detect targets under direct sunlight.

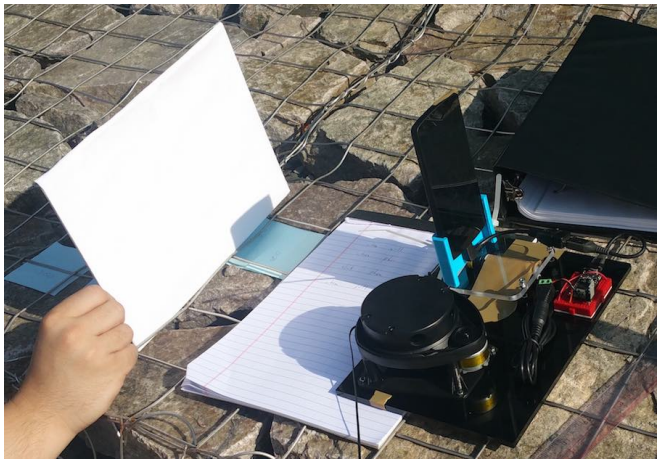

Fig. 9: Experimental setup of Smartphone LDS vs. XV-11.

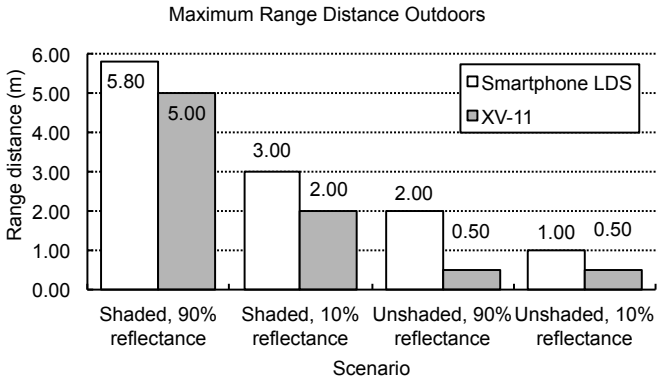

Fig. 10: Maximum range distance comparison.

Smartphone LDS was also unable to obtain range readings at 0.25 m for black targets: the low reflectance combined with undesirable vignetting at the edge of the image caused by our undersized off-the-shelf bandpass filter such that the system could not find bright enough reflected laser light. In our outdoor scenarios, there was unintentional movement of the targets due to wind and hand movements contributing to standard deviation error for both devices.

B. Obstacle Detection Evaluation

We also evaluate our system in an example scenario of obstacle detection for a low-speed autonomous vehicle, mounting it on the front bumper of the testbed vehicle in [1] that is also equipped with a SICK LMS291 LIDAR sensor, used as a baseline. The LMS291 provides a 180 degree field of view, performing measurements at 75 Hz with 10 mm range resolution, +/- 15 mm range accuracy, and 0.25 degree angular resolution. The range of our sensor is limited compared to the LMS291, but can still perform useful obstacle detection for low-speed autonomous vehicles.

Thus, we evaluated the system in three common obstacle avoidance scenarios, illustrated in Figure 13.

1) Obstacle (pedestrian) moving towards and away from front of vehicle.
2) Obstacle (pedestrian) crossing in front of vehicle.
3) Vehicle moving towards and away from stationary object (cardboard box).

Table III shows the minimum distance (out of 5 trials) at which each object was detected in each of the scenarios. We assume instantaneous application of the brakes upon

Fig. 12: Experimental setup for vehicle scenarios.

Preprint submitted to 2016 IEEE International Conference on Robotics and Automation. Received September 15, 2015.

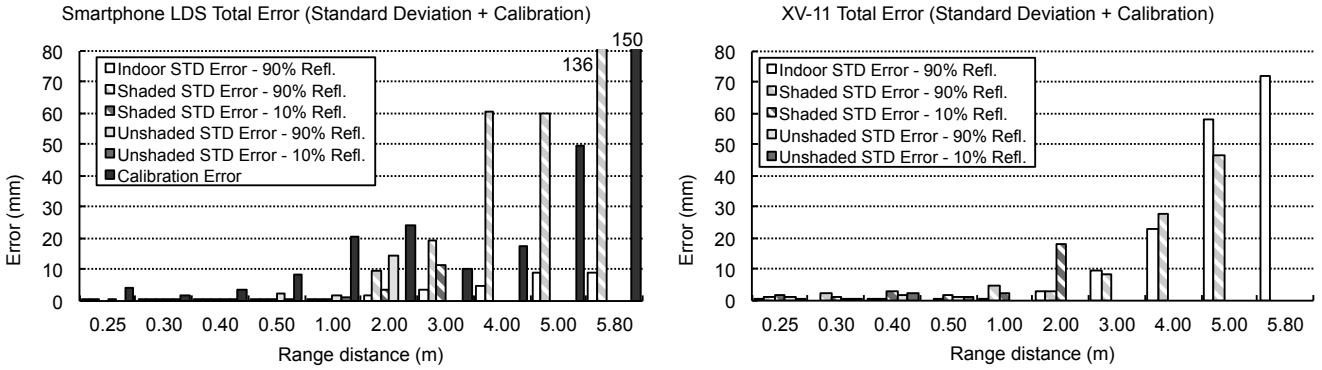

(a) Smartphone LDS error under test scenarios.

(b) XV-11 LDS error under test scenarios.

Fig. 11: Total error comparison.

detection and a comfortable deceleration of $a = 3.4m/s^2$ for collision avoidance [13]. The detection distance is our available vehicle braking distance, and we determine the maximum speed the vehicle can operate at and still avoid collision in Table III with Equation 6 relating stopping distance and constant deceleration.

$$v = \sqrt{2ad} \tag{6}$$

In our experiments, there was significant rolling shutter distortion and vibration in the image due to vibration of the vehicle, to which Smartphone LDS was rigidly attached, which significantly reduced the range compared to Section IV-A because transitions could not be detected. In comparison, the LMS 291 was able to detect the obstacle at all distances tested. However, Smartphone LDS is still able to provide sufficient performance for obstacle avoidance at speeds ranging from 14.8 to 18.5 km/h in the scenarios.

V. Discussion and Conclusion

Our range resolution, angular resolution, maximum range, and detection latency are limited by the performance of the camera sensor and processor performance. The rapid improvement of mobile cameras and processors is the key motivation behind the design of Smartphone LDS, and we discuss the potential improvements that could be realized.

A. Smartphone camera

The CMOS image sensor on the Nexus 5 constrained some aspects of our system performance. To improve it, we would prefer to have:

- **Global shutter.** Our current pulse duration is the duration of the rolling shutter exposure, 33.3 ms. A global shutter would allow a reduction to the image exposure, typically 0.5 to 3 ms, improving maximum range with shorter, higher-power laser pulses and/or improved eye-safety hazard distance. Global shutter cameras targeting computer vision are beginning to appear in mobile devices [15], such as the Amazon Fire Phone [14].
- **High frame-rate.** This reduces detection latency and improves rejection of other periodic signals that might naturally occur in the scene. Many newer phone cameras already support high frame-rates up to 240 frames per second, a 12x improvement, and our exposure time is already low enough to allow these high frame-rates.
- **High dynamic-range.** This prevents sensor saturation by ambient light such that the laser illumination is not detectable, while still allowing us to detect weak laser reflections at long range or on low-reflectance surfaces.

B. Smartphone processor

Our captured image resolution (640 x 480) is well below the full resolution of the image sensor (3264 x 2448) due to image processing bottlenecks, limiting range resolution and angular resolution. Compared to the Snapdragon 800 processor in the Nexus 5, the more recent Snapdragon 810 mobile processor has 113% more CPU performance [7] for a parallelized Sobel kernel (representative of our kernels),

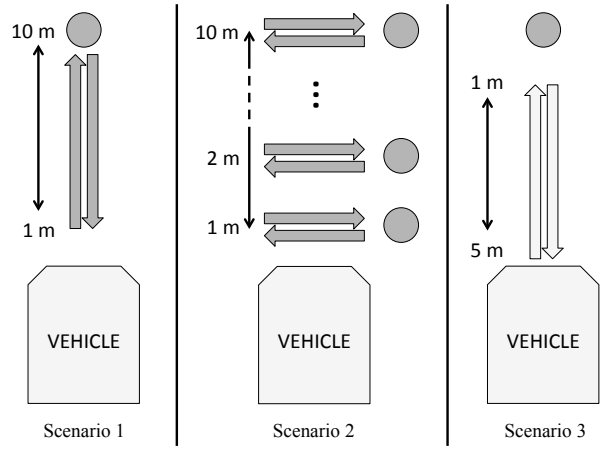

Fig. 13: Diagram of obstacle avoidance scenarios.

TABLE III: Stopping Distance and Corresponding Speed

Scenario	Detection distance	Collision can be avoided under
1	2.5 m	14.8 km/h (4.1 m/s)
2	2.8 m	15.7 km/h (4.4 m/s)
3	3.9 m	18.5 km/h (5.1 m/s)

and 280% more GPGPU performance [18]. Since our image processing is already written as highly parallelized kernels, we estimate that we can at least double the image processing resolution in each dimension just by using a more modern smartphone, doubling minimum angular resolution to 0.05287 degrees as in Equation 3 and doubling range resolution dq by halving dx in the range sensitivity equation [12]:

$$\frac{dq}{dx} = \frac{q^2}{fs} \tag{7}$$

C. Security

Replay attacks have been demonstrated on commercial LIDAR systems [5] by replaying recorded laser illumination patterns. Because the modulation of the laser is controlled by the Smartphone LDS app per-frame, it could use an unpredictable (e.g. pseudorandomly generated) modulation sequence, significantly decreasing the likelihood that maliciously replayed laser illumination will be identified as valid.

D. 3D distance ranging and multi-user ranging

The possibility of using the aforementioned alternate modulation sequence also enables discrimination and identification of multiple lasers in the field-of-view, enabling multiple planes of depth to be sampled, similar to a 3D LIDAR system, and of rejection of unknown signals from other systems operating in the same environment. Using multiple line lasers would restrict the resolution of the additional dimension, while still maintaining high illumination power compared to the limited range of the alternate 3D active illumination depth sensing approaches disucssed in Section II. The Velodyne 3D LIDAR similarly uses multiple laser illumination planes to add the third dimension of distance ranging.

E. Conclusion

We presented a smartphone-based laser distance sensor that is low-cost, solid-state, compact, and works outdoors. The only modifications required to the phone were the addition of a line laser and driver electronics connected to the phone via USB, and a replacement of the camera's infrared-block filter with a band-pass filter. The appearance of infrared-sensitive and global shutter cameras on mobile devices along with silicon advances in phone processors will enable Smartphone LDS to achieve even longer range, and improved eye-safety, readily working with completely unmodified phones by simply attaching a protective phone case with integrated electronics, laser, and filter.

References

[1] ZJ Chong, Baoxing Qin, Tirthankar Bandyopadhyay, Tichakorn Wongpiromsarn, Brice Rebsamen, P Dai, ES Rankin, and Marcelo H Ang Jr. Autonomy for mobility on demand. In *Intelligent Autonomous Systems 12*, pages 671–682. Springer, 2013.

[2] Andrea Colaco, Ahmed Kirmani, Nan-Wei Gong, Tim McGarry, Laurence Watkins, and Vivek K Goyal. 3dim: Compact and low power time-of-flight sensor for 3d capture using parametric signal processing. In *Proc. Int. Image Sensor Workshop*, pages 349–352, 2013.

[3] Michael J Cree, Lee V Streeter, Richard M Conroy, and Adrian A Dorrington. Analysis of the softkinetic depthsense for range imaging. In *Image Analysis and Recognition*, pages 668–675. Springer, 2013.

[4] Office for Research Safety. *Laser safety handbook*. Northwestern University, 2011.

[5] Mark Harris. Researcher hacks self-driving car sensors. `spectrum.ieee.org/cars-that-think/transportation/self-driving/researcher-hacks-selfdriving-car-sensors`, 2015.

[6] Albert S Huang, Matthew Antone, Edwin Olson, Luke Fletcher, David Moore, Seth Teller, and John Leonard. A high-rate, heterogeneous data set from the darpa urban challenge. *The International Journal of Robotics Research*, 29(13):1595–1601, 2010.

[7] Primate Labs Inc. LG Nexus 5 vs HTC One M9. `browser.primatelabs.com/geekbench3/compare/583107?baseline=2326098`, 2014.

[8] Achuta Kadambi, Ayush Bhandari, and Ramesh Raskar. 3d depth cameras in vision: Benefits and limitations of the hardware. In *Computer Vision and Machine Learning with RGB-D Sensors*, pages 3–26. Springer, 2014.

[9] Kourosh Khoshelham and Sander Oude Elberink. Accuracy and resolution of kinect depth data for indoor mapping applications. *Sensors*, 12(2):1437–1454, 2012.

[10] Katsumi Kimoto, Norihiro Asada, Takayoshi Mori, Yoshitaka Hara, Akihisa Ohya, and Shin'ichi Yuta. Development of small size 3d lidar. In *Robotics and Automation (ICRA), 2014 IEEE International Conference on*, pages 4620–4626. IEEE, 2014.

[11] Damon Kohler and Ken Conley. rosjava–An implementation of ROS in pure Java with Android support. `github.com/rosjava/rosjava_core`, 2011.

[12] Kurt Konolige, Joseph Augenbraun, Nick Donaldson, Charles Fiebig, and Pankaj Shah. A low-cost laser distance sensor. In *Robotics and Automation, 2008. ICRA 2008. IEEE International Conference on*, pages 3002–3008. IEEE, 2008.

[13] Akhilesh Kumar Maurya and Prashant Shridhar Bokare. Study of deceleration behaviour of different vehicle types. *International Journal for Traffic and Transport Engineering*, 2(3):253–270, 2012.

[14] David Moloney and Oscar Deniz Suarez. A vision for the future [soapbox]. *Consumer Electronics Magazine, IEEE*, 4(2):40–45, 2015.

[15] OmniVision's Global Shutter CameraCubeChip Brings Computer Vision To Mobile Devices, Notebooks and Wearables. `www.prnewswire.com/news-releases/omnivisions-global-shutter-cameracubechip-brings-computer-vision-to-mobile-devices-notebooks-and-wearables-277202061.html`, 2014.

[16] Annette Payne, Andy Daniel, Anik Mehta, Bradley Thompson, Cyrus S Bamji, Dane Snow, Hirotaka Oshima, Larry Prather, Mike Fenton, Lou Kordus, et al. 7.6 a 512× 424 cmos 3d time-of-flight image sensor with multi-frequency photo-demodulation up to 130mhz and 2gs/s adc. In *Solid-State Circuits Conference Digest of Technical Papers (ISSCC), 2014 IEEE International*, pages 134–135. IEEE, 2014.

[17] Morgan Quigley, Siddharth Batra, Stephen Gould, Ellen Klingbeil, Quoc V Le, Ashley Wellman, and Andrew Y Ng. High-accuracy 3d sensing for mobile manipulation: Improving object detection and door opening. In *ICRA*, pages 2816–2822, 2009.

[18] Anand Lal Shimpi. Qualcomm's Snapdragon 808/810: 20nm High-End 64-bit SoCs with LTE Category 6/7 Support in 2015. `www.anandtech.com/show/7925/qualcomms-snapdragon-808810-20nm-highend-64bit-socs-with-lte-category-67-support-in-2015`, 2014.

[19] Ryan W Wolcott and Ryan M Eustice. Visual localization within lidar maps for automated urban driving. In *Intelligent Robots and Systems (IROS 2014), 2014 IEEE/RSJ International Conference on*, pages 176–183. IEEE, 2014.